Available online at www.sciencedirect.com

SciVerse ScienceDirect

journal homepage: www.elsevier.com/locate/acme

Original Research Article

Determination of the friction coefficient as a function of sliding speed and normal pressure for steel C45 and steel 40HM ☆

*M. Stembalski**, *P. Preś*[1], *W. Skoczyński*[2]

Wrocław University of Technology, Lukasiewicza 5 Street, Building B-4, Poland

ARTICLE INFO

Article history:
Received 12 July 2012
Accepted 26 April 2013
Available online 10 May 2013

Keywords:
Coefficient of friction
Tests
Analytical model
Numerical analysis

ABSTRACT

This paper presents a method of determining the coefficient of friction as a function of sliding speed and normal pressure for different friction pairs of materials used in friction dampers. A schematic of the experimental setup is shown and the course of the experiment is described. An analytical relation describing the influence of sliding speed and normal pressure on the friction coefficient for C45 and 40HM steel was derived. Then on the basis of the analytical relation 3D numerical models were created. Computations using the Abaqus/Standard software package were performed.

1. Introduction

In order to model such systems as friction dampers or brakes by means of finite elements one needs to know the friction coefficient as a function of selected parameters (e.g. sliding speed, normal pressure, etc.). It is necessary to determine function $\mu = f(\rho, \dot{\gamma})$ to properly represent the contact between the interacting parts. In many cases, the usually employed model with the exponential attenuation of the friction coefficient is insufficient. Numerous studies [6,8,9,11,15,21,22] have shown that the friction coefficient to a large extent depends on the normal pressures. Therefore the authors decided to determine the friction coefficient as a function of normal pressure and sliding speed. The results presented in this paper will be used in the future for more accurately modeling the contact components in the friction damper model.

The friction force is defined as a force counteracting the relative motion of two contacting bodies. The friction force has a direction tangent to the surface of the contact and a sense opposite to the sense of the velocity of motion of one body relative to the other body. According to the generally used Coulomb model, friction force F_t is directly proportional to normal force F_n and to constant friction coefficient μ:

$$F_t = \mu F_n \tag{1}$$

Numerous experimental studies have shown that as the sliding speed, the normal pressures, the temperature and other unspecified factors increase, the value of friction coefficient μ changes nonlinearly [1–5,10,12,15,16,17]. Each material has its singular graph of function μ, which in a general form can be written as

$$\mu = f(\rho, \dot{\gamma}, T, f^{\alpha}) \tag{2}$$

☆Financial disclosure: Own research 2011 no B10041F, statutory funding Zakład Obrabiarek i Systemów Mechatronicznych, Wrocław University of Technology.

*Corresponding author. Tel.: +48 71 320 21 77; fax: +48 71 320 2701.
E-mail address: marek.stembalski@pwr.wroc.pl (M. Stembalski).
[1]Tel.: +48 71 320 21 77.
[2]Tel.: +48 71 320 26 39.

1644-9665/$ - see front matter © 2013 Published by Elsevier Urban & Partner Sp. z o.o. on behalf of Politechnika Wrocławska.
http://dx.doi.org/10.1016/j.acme.2013.04.010

where ρ is the normal pressure, $\dot{\gamma}$ is the sliding speed, T is the temperature and f^{α} are other unspecified factors.

Knowing the curve of the friction coefficient versus the above variables one can more precisely predict the value of the tangent force and that of the dissipated energy, produced by friction between two bodies moving relative to each other.

It was shown in many studies [1–5,9] that for most materials the friction coefficient at a sliding speed equal to zero is higher than the one during sliding. This observation is expressed by an exponential model described by the following relation [13]:

$$\mu = \mu_k + (\mu_s - \mu_k)e^{-d_c\dot{\gamma}} \tag{3}$$

where μ_k is a coefficient of kinetic friction, μ_s is a coefficient of static friction, and d_c is a coefficient of attenuation.

The equation with the exponential attenuation of the friction coefficient is often used in finite element modeling [7,9]. The theoretical curve of friction coefficient versus sliding speed is shown in Fig. 1.

However, in many cases the model with friction coefficient exponential attenuation is insufficient. Numerous studies [6,8,9,11,18,19] have shown that the friction coefficient to a large extent depends on the normal pressures. The theoretical relation between friction coefficient and normal pressure is shown in Fig. 2. The accuracy of friction force estimation increases when the normal load is taken into account.

Therefore the authors decided to make an attempt to determine the friction coefficient as a function of sliding speed $\dot{\gamma}$ and normal pressure ρ in order to incorporate the derived relation into the numerical model of the passive friction damper.

2. Experimental setup and course of experiment

The coefficient of friction as a function of sliding speed and normal pressure was determined for steel C45 and steel 40HM.

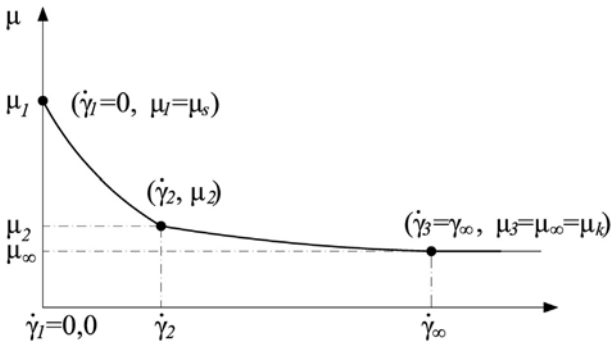

Fig. 1 – Exponential model describing dependence between friction coefficient and sliding speed [7,20].

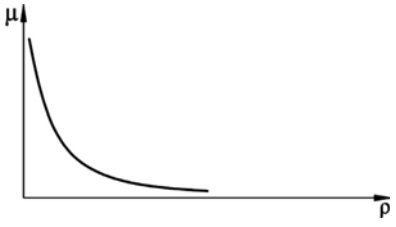

Fig. 2 – Friction coefficient versus normal pressure.

The materials were not toughened. C45 and 40HM steels were used to build a friction damper. As a result of relative vibrations between the contacting surfaces the damper frictional components cause the energy of the vibrations to dissipate. Therefore it is necessary to determine the dependence $\mu = f(\rho, \dot{\gamma})$ for the materials of the damper frictional parts in order to accurately model the contact between them.

The open linear tribologic system model [2,3] was used to determine the friction coefficient. A 100 mm wide and 150 mm long plate constituted the flat surface. A cylindrical pin 20 mm in diameter constituted the counter sample. In the course of the experiment the pin face was pressed against the plate's flat surface with a specified force (Fig. 3).

A NC milling machine was used in the experiment. The milling machine's design and drive permitted the motion of the cylindrical pin relative to the plate's surface at a programmed speed and change of the force pressing down the pin to the plate. As a result of the movement of the milling machine table along axis X of the machine tool coordinate system (Fig. 3) one of the elements moved relative to the other. In all tests the friction distance was 80 mm. Thanks to the movement of the milling machine's spindle along axis Z (Fig. 3) the force pressing down the pin to the flat surface of the sample could be changed. The force was changed from 100 to 400 N. The sliding speed changed in a range of 0–5 mm/s. The range of measured values of normal load and sliding velocity was taken from earlier research on friction damper. The research showed that normal pressure and sliding velocity during working of prototype friction damper changes in the range from 0.393 to 1.286 MPa for normal load and from 0 to 5 mm/s for sliding velocity.

The change of the speed over time is shown in Fig. 4. The rate of travel of the milling machine table along axis X was changed stepwise through the control program. The rate of feed increased by 0.0025 mm/s for each covered distance length of 0.04 mm. The load and speed ranges coincide with the possible operating ranges of the friction damper.

The interacting surfaces of the samples were grinded. The roughness of the rubbing surfaces of the frictional elements was measured by means of a Taylor-Hobson Form Talysurf 120L surface analyzer. The results of the measurements are presented in Table 1.

To carry out the experiments a NC milling machine was used. It was decided by the three considerations. This machine was

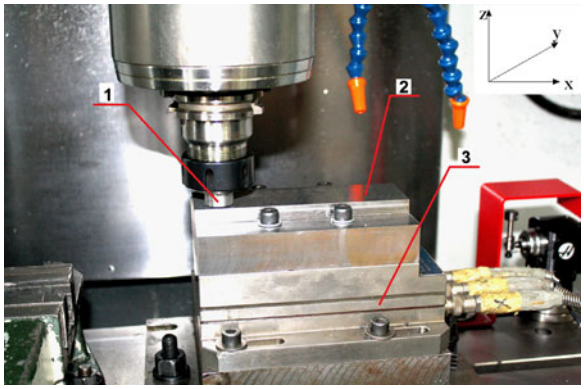

Fig. 3 – Interacting rubbing surfaces: 1—cylindrical rubbing pin, 2—sample with flat rubbing surface, 3—triaxial piezoelectric force gauge KISTLER type 9257A.

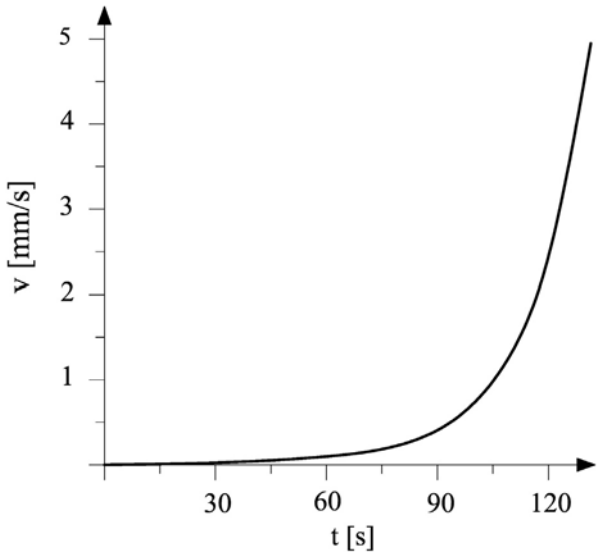

Fig. 4 – Exemplary graph of sliding speed versus time.

Table 1 – Results of rubbing surfaces roughness measurements.

Material	Rubbing pin Ra (μm)	Plate Ra (μm)
C45	0.49	0.08
40HM	0.23	0.09

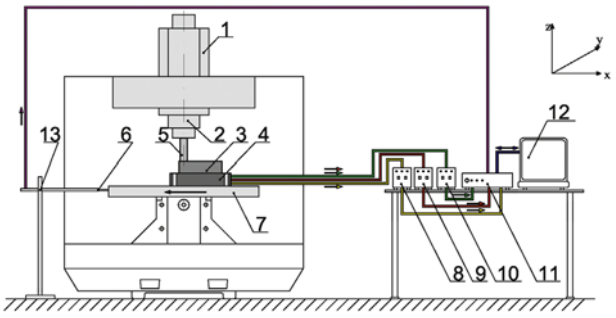

Fig. 5 – Schematic of experimental setup for determining friction coefficient: 1—milling machine HAAS type TH1P, 2—milling machine spindle, 3—flat-surface test specimen, 4—three-axis piezoelectric force gauge KISTLER type 9257A, 5—cylindrical rubbing pin, 6—displacement sensor HBM type WA100, 7—milling table, 8, 9, 10—charge amplifiers KISTLER type 5011 (axes X, Y, Z), 11—measuring system Spider 8, 12—laptop, 13—displacement sensor stand.

equipped with a drive that allowed the control of the sliding speed changes of rubbing pin relative to the plate. Whereas a geometric accuracy of the machine enabled maintaining parallel direction of slip relative to this plate. Milling spindle was served only to fix the rubbing pin and did not rotate during experiment. A control unit of the machine allowed also the setting of the specific normal force. The course of sliding speed rising was due to the machine control unit properties.

In order to find out how friction coefficient μ changes depending on pressure ρ and sliding speed $\dot{\gamma}$ (Fig. 5) the plate (3) was placed on the triaxial piezoelectric force gauge (4) mounted on the milling machine table (7). The cylindrical rubbing pin was installed in the milling machine spindle (2). In the course of the tests the normal force (along the Z axis) and the tangent force (along the X axis) were measured. The signals from the force gauge's particular axes were transmitted to the KISTLER type 5011 charge amplifiers (8–10). After amplification the signals were directed to the Spider 8 measuring system (11). A laptop with the Catman (ver. 3) software was used for communication with the measuring system. The displacement of the milling machine table (6) was measured by the HBM type WA100 displacement transducer. The signal from the sensor was sent directly to a Spider 8 type amplifier (11) [14] and recorded. Then, in off line mode the measured signal was differentiated in order to obtain the speed signal. All measurements were performed for the same sampling frequency of 600 Hz.

3. Measurement results

Exemplary courses of normal and tangential forces, and displacements, recorded during a full test at a load of 0.65 MPa for 40HM steel are shown in Fig. 6a. At the beginning of the test, rubbing pin is pressed against the plate and the normal force increases to a constant value of about 200 N.

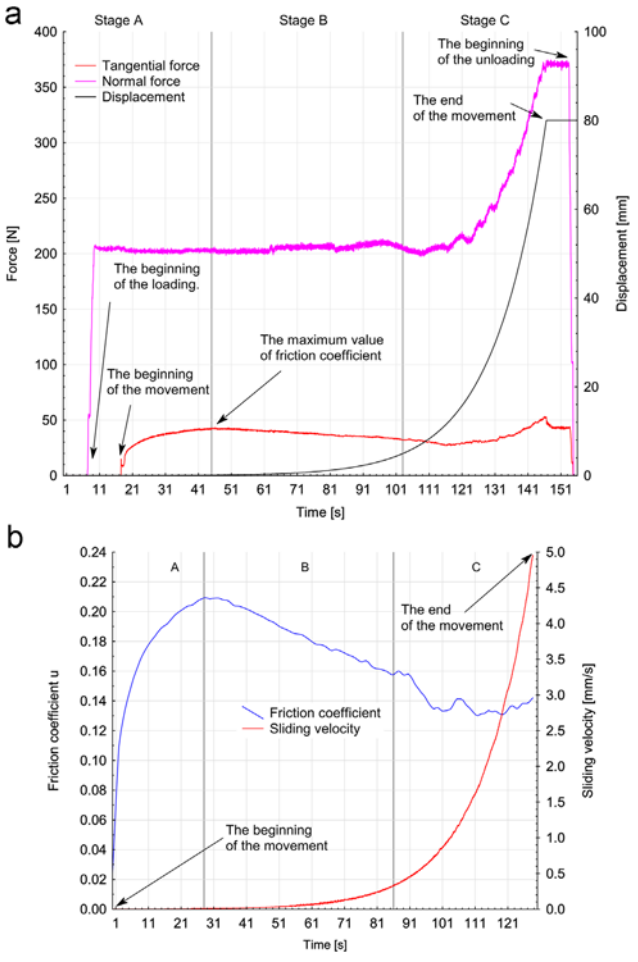

Fig. 6 – Exemplary results at load of 0.65 MPa: (a) time courses of measured normal and tangential forces and relative displacements and (b) time courses of the coefficient of friction and sliding speed determined from measurements.

After stabilization of the normal force, a relative motion of contacting surfaces begins, with a gradually rising sliding speed. Tangential force initially increases along with an increase in the preload of the milling machine structure and reaches a maximum, probably related to the static friction force. With the increasing sliding speed, the friction force decreases, but upon reaching a certain speed, it starts to rise again. It is related to a large increase in the normal force. This is probably area of flat surface cutting, using the edge of rubbing pin.

Based on the characteristics of registered tangential and normal forces, the friction coefficient μ was determined (Fig. 6b). The characteristics of relative displacements were differentiated and thus, courses of the sliding speed were calculated. The stage B of the friction coefficient curve was chosen for further analysis. This stage covers an area of constant normal load ρ from the threshold of motion point (Fig. 6a). Two other stages were excluded from the analysis. In stage A, the friction coefficient μ increases to the maximum value, which corresponds to the threshold of motion. Friction conditions change also in stage C, where the normal force significantly increases. Therefore, only in stage B constant friction conditions were kept. Fig. 7 shows the obtained fragments of the waveforms for different constant normal loads for steel 40HM. These waveforms shown in Fig. 7 were used to determine (for each case of normal pressure) the dependences described by general function $\mu = f(\dot{\gamma})$. The experimentally determined curves (Fig. 7), representing the friction coefficients as a function of sliding speed, were approximated by the following trend function:

$$\mu = a + be^{\dot{\gamma}c} \tag{4}$$

Fig. 8 shows several curves of function (4) for different normal pressures. The dependence between friction coefficient μ and sliding speed $\dot{\gamma}$ was determined for different constant normal pressure ρ values from the range of 0.393 to 1.286 MPa. Seven functions in exponential form (4) were obtained.

The Statistica (ver. 10) software package was used to take into account the influence of normal pressure values and to derive a single analytical relation expressing the influence of $\dot{\gamma}$ on friction coefficient μ in the assumed interval of sliding speed and normal pressures ρ.

The quasi-Newton nonlinear estimation method was employed and least squares regression lines were fit to the data. Using function form (4) the values of parameter a for C45 steel and those of parameters a and c for 40HM steel were interrelated with the normal pressure value. The influence of normal pressure on the friction coefficient was determined. The change in parameter a with increasing normal pressure was expressed through an exponential function. The change in parameter c for 40HM steel was described by a logarithmic function.

The following two equations expressing the influence of sliding speed and normal pressure on the friction coefficient were derived:

$$\mu = 0.2e^{-0.375\rho} + 0.046e^{(-(-1.84\ln(\rho)+8.42)\dot{\gamma})} \text{ for 40HM steel} \tag{5}$$

$$\mu = 0.179e^{-0.16\rho} + 0.074e^{-18.62\dot{\gamma}} \text{ for C45 steel} \tag{6}$$

The value of determination coefficient R^2 for 40HM steel was equal to 0.942. The value of determination coefficient R^2 for C45 steel was equal to 0.84.

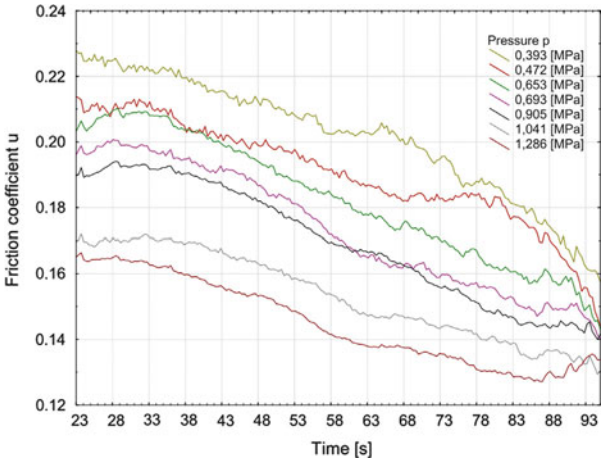

Fig. 7 – Narrowed down friction coefficient μ waveforms for different normal pressures ρ.

4. Numerical model

The analytical relations presented in this paper were implemented in numerical models. They were created using FEM

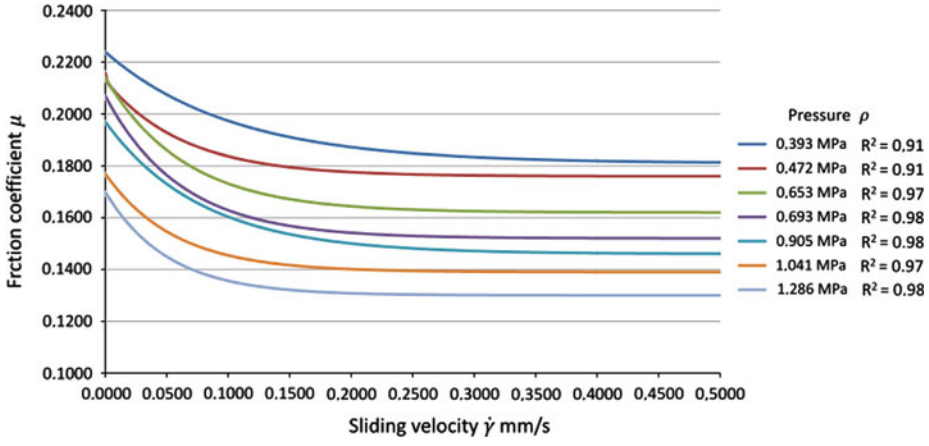

Fig. 8 – Friction coefficient μ as the experimental function of sliding speed γ and normal pressure ρ for 40HM steel interfaces.

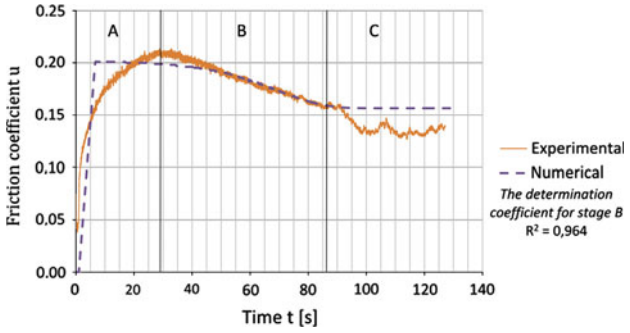

Fig. 9 – Comparison of exemplary friction coefficient curves at a pressure of 0.653 MPa for 40HM steel, obtained using experimental model and numerical model.

and the Abaqus/Standard software package. Fig. 9 shows the friction coefficient values for 40HM steel calculated from the experimental data. They were compared with the ones obtained from FEM simulations at the normal load of 0.653 MPa.

As it appears from the above, when the analytical relations were introduced into the model created using FEM, the model showed high agreement with the experimental results (Fig. 9 stage B). Thus one can say that the derived analytical relations correctly describe the correlation between the friction coefficient and sliding speed and normal pressure ρ. The relations can be used to model contact parts in friction dampers made of C45 and 40HM steel.

5. Conclusion

The results of experimental research confirmed the effect of normal pressure and sliding speed of contacting surfaces on the friction coefficient. When besides sliding speed, normal pressure is taken into account, the accuracy of estimating the tangent force increases. The designated analytical models are useful in numerical modeling of contact phenomena. The models can be used to build a numerical model of the friction damper.

REFERENCES

[1] J. Rech, C. Claudin, E. Eramo, Identification of a friction model—application to the context of dry cutting of an AISI 1045 annealed steel with a TiN-coated carbide tool, Tribology International 42 (2009) 738–744.
[2] C. Bonnet, F. Valiorgue, J. Rech, C. Claudin, Identification of a friction model—application to the context of dry cutting of an AISI 316L annealed steel with a TiN-coated carbide tool, International Journal of Machine Tool & Manufacture 48 (2008) 1211–1223.
[3] O. Klinkova, J. Rech, S. Drapier, J.-M. Bergheau, Characterization of friction properties at the workmaterial/cutting tool interface during the machining of randomly structured carbon fibres reinforced polymer with carbide tools under dry conditions, Tribology International 44 (2011) 2050–2058.
[4] C. Claudin, A. Mondelin, F. Dumont, J. Rech, Effects of lubrication mode of friction and heat partition coefficients at the tool–workmaterial interface in machining, in: Proceedings of the Eight International Conference on High Speed Machining, 2010, pp. 156–164.
[5] L. Liang, Q. Baoyun, H. Ning, Antifriction action of cooling and lubrication media on Ti6A14V/WC-Co, in: Proceedings of the Eight International Conference of High Speed Machining, 2010, pp. 151–154.
[6] L. Filice, F. Micari, S. Rizutti, D. Umbrello, A critical analysis of the friction modelling in orthogonal machining, International Journal of Machine Tool & Manufacture 47 (2007) 709–714.
[7] W. Miszczak, The determination of the friction coefficient on the face within the drill cutting edge area for the FEM modelling of chip formation (in Polish), Scientific Papers of the Machine Building Department, Silesian Polytechnic, Gliwice, 2008, pp. 103–112.
[8] J. Brocail, M. Watremez, L. Dubar, Identification of a friction model for modelling of orthogonal cutting, International Journal of Machine Tools and Manufacture 50 (2010) 807–814.
[9] F. Zemzemi, J. Rech, W. Ben Salem, A. Dogui, P. Kapsa, Identification of the friction model at tool/chip/workpiece interfaces in dry machining of AISI4142 treated steel, Journal of Materials Processing Technology 209 (2009) 3978–3990.
[10] W. Grzesik, P. Nieslony, Prediction of friction and heat flow in machining incorporating thermophysical properties of the coating–chip interface, Wear 256 (2004) 108–117.
[11] E. Kwiatkowska, The influence of friction in fem simulation of chip formation, Advances in Manufacturing Science and Technology 32 (2) (2008) 39–51.
[12] P. Naisson, J. Rech, H. Paris, Characterization of friction properties during machining of various stainless steels, in: Proceedings of the Eight International Conference on High Speed Machining, 2010, pp. 115–120.
[13] Abaqus.6.9 Software Documentation.
[14] Hottinger Baldwin Messtechnik: Spider 8 Amplifier and Catman Software Technical Documentation. ⟨http://www.hbm.com⟩.
[15] M. Chen, K. Kato, K. Adachi, The comparison of sliding speed and normal load effect on friction coefficient of self-mated Si_3N_4 and SiC under water lubrication, Tribology International 35 (2002) 129–135.
[16] P. Spijker, G. Anciaux, J. Molinari, Relations between roughness, temperature and dry sliding friction at the atomic scale, Tribology International 59 (2012) 222–229.
[17] E. Feyzullahoglu, Z. Saffak, The tribological behaviour of different engineering plastics under dry friction conditions, Materials and Design 29 (2008) 205–211.
[18] R. Tyagi, D. Xiong, J. Li, Effect of load and sliding speed on friction and wear behaviour of silver/h-BN containing Ni-base P/M composites, Wear 270 (2011) 423–430.
[19] J. Yang, W. Gu, L.M. Pan, K. Song, X. Chen, T. Qui, Friction and wear properties of in situ (TiB_2+TiC)/Ti_3SiC_2 composites, Wear 271 (2011) 2940–2946.
[20] J.T. Oden, J.A.C. Martins, Models and computational methods for dynamic friction phenomena, Computer Methods in Applied Mechanics and Engineering 52 (1985) 527–634.
[21] M.A. Chowdury, M.K. Khalil, D.M. Nuruzzaman, M.L. Rahaman, The effect of sliding speed and normal load on friction and wear property of aluminium, International Journal of Mechanical & Mechatronics Engineering IJMME-IJENS 11 (2011) 53–57.
[22] A. Yasuhisa, Lowering friction coefficient under low loads by minimizing effects of adhesion force and viscous resistance, Wear 254 (2003) 965–973.